

Effect of Charge Density on the Dynamic Behavior of Polyelectrolytes in Aqueous Solution

A. Topp, L. Belkoura, and D. Woermann*

Institut für Physikalische Chemie, Universität Köln, Luxemburger Strasse 116, D-50939 Köln, Germany

Received February 21, 1996

ABSTRACT: Dynamic light scattering experiments and measurements of surface tension and viscosity of aqueous solutions of poly(2-vinylpyridine) quaternized with ethyl bromide are carried out as function of the charge density and polyelectrolyte concentration ($M_w = 2.9 \times 10^5$, $M_w/M_n = 1.11$; α_e , degree of quaternization, $0.09 \leq \alpha_e \leq 0.46$). The polyelectrolytes are dissolved in an aqueous solution of potassium bromide ($c_s = 1 \times 10^{-2} c^+$, $c^+ = 1 \text{ mol dm}^{-3}$). Their concentrations \bar{c}_p are in the range $0.1 \bar{c}^+ \leq \bar{c}_p \leq 27 \bar{c}^+$ ($\bar{c}^+ = 1 \text{ g dm}^{-3}$). The reduced variable $\Lambda (= \alpha_e c_m / c_s)$ is used to characterize the composition of the solutions (c_m , molar volume concentration of the repeat unit of the polymer backbone). Monomodal and bimodal dynamic modes characterized by the apparent diffusion coefficients D_s and D_f (index s, slow; index f, fast) are found under the following conditions: monomodal, $0.03 \leq \Lambda \leq 0.1$; bimodal, $0.1 \leq \Lambda \leq 8$. A third dynamic mode characterized by the apparent diffusion coefficient D_{int} (index int, intermediate) appears at $\Lambda \geq 1$ with small values of α_e in the range $0.09 \leq \alpha_e \leq 0.15$ ($D_s < D_{\text{int}} < D_f$). It is assumed that the third mode reflects dynamic properties of hydrophobic domains formed by uncharged segments of the polymer backbone at low values of α_e . Hydrophobic interactions show up also in surface tension and viscosity measurements. A model proposed by Lee and Schurr (*J. Polym. Sci.* **1975**, *13*, 873) describes the experimental D_f data of the fast diffusive mode with two fit parameters (Z_{eff} , effective number of charges of a polyion; D_p , diffusion coefficient of a polyion). Z_{eff} is smaller by a factor of 5–7 than the value calculated on the basis of α_e .

1. Introduction

The dynamics of polyelectrolytes with high charge density in aqueous electrolyte solutions have been studied extensively using the dynamic light scattering technique.^{1–3} In the presence of a 1, –1 valent electrolyte in the solutions, the dynamic properties are known to be a function of the concentration ratio $\lambda (= c_m / c_s$; c_m is the molar volume concentration of charged monomer units of the polyelectrolyte and c_s the molar volume concentration of the electrolyte). The analysis of the autocorrelation function of the scattered light intensity leads to the apparent diffusion coefficient D . A characteristic not sharply defined value λ^* is found which divides a double-logarithmic $D(\lambda)$ diagram of experimental data into two regions.^{3,4} For values of $\lambda < \lambda^*$ the autocorrelation function is monomodal, corresponding to a single apparent diffusion coefficient. It becomes bimodal for values of $\lambda > \lambda^*$, with two apparent diffusion coefficients D_f and D_s characterizing a “fast” and “slow” diffusive mode. Approaching λ^* from values $\lambda > \lambda^*$, the fast mode slows down. The slow mode becomes faster and disappears at λ^* . For values of $\lambda \approx \lambda^*$ the fast mode goes over to the single mode observed at $\lambda < \lambda^*$. The dependence of the fast apparent diffusion coefficient D_f on λ ($\lambda \geq \lambda^*$) can be described by the “coupled mode theory” worked out by Lee and Schurr.^{5,6} The physics causing the slow mode is not fully understood yet.

It is the aim of this study to extend dynamic light scattering experiments to well-defined polyelectrolyte systems with low charge densities in aqueous solution. The polyelectrolytes are prepared by changing the degree of quaternization of poly(2-vinylpyridine) (P2VP) with ethyl bromide (α_e , degree of quaternization with ethyl bromide). Starting from values just large enough to make P2VP dissolvable in a dilute electrolyte solution ($\alpha_e \approx 0.08$; $c_s(\text{KBr}) = 1 \times 10^{-2} c^+$, $c^+ = 1 \text{ mol dm}^{-3}$), the

values of α_e are increased until a further increase does not influence the dynamics of the polyelectrolyte in any specific way ($\alpha_e = 0.46$). A degree of quaternization of $\alpha_e = 0.35$ leads to a mean distance between two pyridinium groups $\langle L \rangle = 0.7 \text{ nm}$ corresponding to the Bjerrum length $l_B (= e^2 / (\epsilon k_B T))$, $l_B = 0.71 \text{ nm}$; ϵ , dielectric constant; k_B , Boltzmann's constant). This value of $\langle L \rangle$ is the minimum distance of charges above which counterion condensation occurs.⁷ The concentration of the added salt is kept constant at a value $c_s = 1 \times 10^{-2} c^+$.

This method to prepare polyelectrolytes with low charge density is considered preferable to the method described in the literature which consists of changing the charge density of polyelectrolytes by adding acid or base to uncharged polymers with groups that can be ionized.^{8,9} The quaternization of P2VP with ethyl bromide makes it possible to determine the value of α_e accurately by elementary analysis of nitrogen and bromide.¹⁰

A change of the degree of quaternization at low values of α_e results in a change of the hydrophobic/hydrophilic balance of the P2VP polyelectrolytes. This is an alternative to a complete quaternization of P2VP with varying the degrees of alkyl bromides α_{alk} (e.g., dodecyl bromide) and ethyl bromide α_e or varying the length of alkyl side groups at fixed values of α_{alk} and α_e .^{11–13}

2. Experimental Section

Quaternization. P2VP with a narrow molar mass distribution determined by exclusion chromatography ($M_n = 2.57 \times 10^5$; $M_w = 2.87 \times 10^5$; $M_w/M_n = 1.11$) was purchased from Polymer Standards (Mainz, Germany). The material was received in a freeze-dried state and was used without further purification.

Six samples of P2VP were dissolved in mixtures of nitromethane/nitroethane (volume ratio 2.5:1) and quaternized with ethyl bromide at a reaction temperature $T_r = 40.0 \pm 0.1^\circ \text{C}$.¹⁰ The degree of quaternization with ethyl bromide α_e was varied by varying the reaction time t_r ($19 \text{ h} \leq t_r \leq 744 \text{ h}$; $0.09 \leq \alpha_e \leq 0.46$). α_e was determined by elementary analysis ($\alpha_e = (n_{\text{Br}} /$

* To whom correspondence should be addressed.

© Abstract published in *Advance ACS Abstracts*, June 15, 1996.

Table 1. Characterization of the P2VP Samples Used in This Study: α_e , Degree of Quaternization with Ethyl Bromide; $M_{n,e}$, Number-Average Molar Mass of the Quaternized Sample; Z , Number of Quaternized Pyridine Groups of One Polymer Chain (Calculated Using M_n); $\langle L \rangle$, Average Linear Distance between Two Quaternized Pyridine Groups along the Polymer Chain ($\langle L \rangle = l_0/\alpha_e$; l_0 , Length of One Monomer Unit; $l_0 = 0.25$ nm)

α_e	$M_{n,e}/10^{-5}$ ^a	Z	$\langle L \rangle/\text{nm}$
0.09	2.81	220	2.8
0.10	2.84	250	2.5
0.12	2.89	290	2.1
0.15	2.97	370	1.7
0.22	3.16	540	1.1
0.46	3.80	1120	0.5

^a $M_{n,e}$ is calculated by using the expression $M_{n,e} = M_w + (M_n\alpha_e/M_e)/M_{\text{mono}}$ (M_n , number-average molar mass of the uncharged P2VP; M_{mono} , molar mass of an unquaternized monomer unit, $M_{\text{mono}} = 105.14$; M_e , molar mass of ethyl bromide, $M_e = 108.97$; α_e , degree of quaternization with ethyl bromide).

n_i ; n_i amount of substance of species i ; Pascher, Remagen-Bandorf, Germany). The data characterizing the samples are given in Table 1.

Preparation of the Aqueous Polyelectrolyte Solutions.

The polyelectrolyte solutions were prepared by dissolving a known mass of the polyelectrolyte in its dried state in less than the required volume of the aqueous solution of KBr ($c_s = 1 \times 10^{-2} \text{ c}^+$). The dissolution of the polyelectrolyte took about 12 h. Finally, the KBr solution was added in order to obtain the desired polyelectrolyte concentration. Before use the solutions were filtered through a pore-controlled polycarbonate filter with a pore size of $0.22 \mu\text{m}$ (Millipore, Eschborn, Germany).

Surface Tension. The air/water surface tension σ was measured with a digital tensiometer K 10ST (Krüss, Hamburg, Germany) with a reproducibility of $\delta\sigma = \pm 0.1 \text{ mN m}^{-1}$ using a Wilhelmy plate. The experiments were carried out at four temperatures in the range $20^\circ\text{C} \leq T \leq 50^\circ\text{C}$ ($\delta T = \pm 0.1^\circ\text{C}$) at a constant mass concentration of the polyelectrolyte ($\bar{c}_p = 1\text{c}^+$; $c_s = 1 \times 10^{-2} \text{ c}^+$; $\bar{c}^+ = 1 \text{ g dm}^{-3}$). Before each measurement, the solution was stirred rigorously. σ was measured as function of time using a recorder. The surface tension reached a time-independent value after about 2.5 h at the longest. The solutions of polyelectrolytes with small values of α_e required longer time to reach time-independent values of σ .

Viscosity. The viscosity measurements were carried out with an Ubbelohde viscometer of the dilution type (Schott, Hofheim a. Ts., Germany; Type 53101; r_c , radius of the capillary, $r_c = 0.27 \text{ mm}$; $\langle \Delta h \rangle$, mean height of the liquid column, $\langle \Delta h \rangle = 130 \text{ mm}$; L , length of the capillary, $L = 90 \text{ mm}$) in combination with an optical detection system (Schott; Type AVS 350). The measured efflux times t were corrected for the kinetic energy effect. The effective shear rate was calculated using the relation $S_{\text{eff}} = (4/15)[\rho g \langle \Delta h \rangle r_c / (\eta L)]$ (ρ , density of the solution; g , acceleration caused by gravity; η , viscosity of the solution).¹⁴ The intrinsic viscosity $[\eta]$ of the aqueous polyelectrolyte solutions was determined from viscosity data obtained in a concentration range $1.5\bar{c}^+ \leq \bar{c}_p \leq 6.0\bar{c}^+$ ($[\eta] = \lim_{\bar{c}_p \rightarrow 0} \{(\eta - \eta_0)/\eta\}/\bar{c}_p$; η and η_0 , viscosity of the polyelectrolyte and the KBr solution, respectively).

Dynamic Light Scattering. Light Scattering Photometer.

A home-built light scattering goniometer was used for the experiments similar to that described elsewhere.¹⁵ The accessible scattering angles θ were in the range $30^\circ \leq \theta \leq 140^\circ$ ($\delta\theta = \pm 0.01^\circ$). The light source was an argon-ion laser (Spectra Physics, Model 2020) with a maximum output of 1 W at the wavelength 488 nm. In the light scattering experiments it was operated at about 150 mW. The beam intensity was adjusted according to the scattering power of the samples. The long-time temperature stability of the samples in the goniometer was $\delta T < 1 \text{ mK}$. The scattered light intensity was measured with a Malvern photomultiplier assembly (Model PC55) used in combination with a discriminator BI-PAD (Brookhaven Instruments Co.). The autocorrelation function of the scattered light was measured with a digital correlator (Brookhaven Instruments Co., Model 9000K) operating in the delay time limits $10^{-7} \text{ s} \leq \tau \leq 1 \text{ s}$.

Sample Preparation for the Dynamic Light Scattering Experiments. The procedure to prepare the samples used for the dynamic light scattering experiments was described before.¹⁰ Prior to the measurements, the flame-sealed scattering cells were centrifuged for 2 h at 2000g.

Data Acquisition and Data Analysis. The autocorrelation function $G^{(2)}(\tau) (= \langle n(t) n(t+\tau) \rangle)$; τ , delay time) of light scattered at a scattering vector q is measured by the autocorrelator ($0.88 \times 10^5 \text{ cm} \leq q \leq 3.3 \times 10^5 \text{ cm}^{-1}$; $30^\circ \leq \theta \leq 140^\circ$; $q = (4\pi n/\lambda_0) \sin(\theta/2)$; λ_0 , wavelength of incident light in vacuum; n , refractive index of the solution). $G^{(2)}(\tau)$ is measured at each scattering angle up to 50 times (50 runs) for a duration of 120 s. These runs form a set. The correlation function of each run of a set is converted into the normalized second-order correlation function $g^{(2)}(\tau)$ using the relation $g^{(2)}(\tau) = G^{(2)}(\tau)/B$. The value of the infinite-time baseline B is given by $B = N_{\text{total}}/N_s$ (N_s , number of sample times Δt during which photon counts are recorded; N_{total} , total number of photon counts recorded during the run). To eliminate runs of a set affected by the scattering of dust particles, the mean value $\langle N_{\text{total}} \rangle$ of the set of runs is calculated together with the relative deviation $\Delta N_{\text{total},i}$ of each run from the mean value (i.e., $\Delta N_{\text{total},i} = (N_{\text{total},i} - \langle N_{\text{total}} \rangle)/\langle N_{\text{total}} \rangle$). Run i of a given set of runs with the largest value of $N_{\text{total},i}$ is eliminated from further considerations when $\Delta N_{\text{total},i}$ is larger than a preset value of the relative deviation $(\Delta N_{\text{total}})_{\text{max}}$. The choice of the value of $(\Delta N_{\text{total}})_{\text{max}}$ depends on the scattering angle and the scattered light intensity (e.g., $0.01 \leq (\Delta N_{\text{total}})_{\text{max}} \leq 0.05$). This procedure is repeated until each run of a set satisfies the relation $\Delta N_{\text{total},i} \leq (\Delta N_{\text{total}})_{\text{max}}$. From the selected runs the value of the normalized second-order correlation function $g^{(2)}(\tau)$ is calculated. Also calculated is the standard deviation s_τ for each delay time τ ($80 \leq n_\tau \leq 220$; n_τ , number of delay times). From the mean value of $g^{(2)}(\tau)$ the normalized electric field autocorrelation function $g^{(1)}(\tau)$ is obtained using the relation $g^{(1)}(\tau) = (g^{(2)}(\tau) - 1)^{1/2}/\beta$. For the calculation the coherence factor β is set to $\beta = 1$.

In a solution of polyelectrolytes several processes with different relaxation rates Γ are expected to contribute to $g^{(1)}(\tau)$. The distribution function $A(\Gamma)$ of the amplitudes of Γ and $g^{(1)}(\tau)$ are related by eq 1. Solving eq 1 for $A(\Gamma)$ is known as Laplace

$$g^{(1)}(\tau) = \int_0^\infty A(\Gamma) \exp\{-\Gamma\tau\} d\Gamma \quad (1)$$

inversion. The conversion is carried out with Provencher's program CONTIN (version 2DP).^{16,17} It was applied in the following way:

(a) The source code of the program is modified to set the number of grid points (CONTIN-parameter NG) from 44 to 70 in order to improve the resolution of $A(\Gamma)$.¹⁸ This is advantageous because $A(\Gamma)$ in the systems studied covers a wide range ($10^{-7} \text{ s} \leq \tau \leq 1 \text{ s}$).

(b) The experimentally determined standard deviations s_τ of the delay times are used in the calculation of $A(\Gamma)$ (i.e., CONTIN-parameter IWT = 4).

(c) The program CONTIN with the parameter IQUAD set to IQUAD = 3 leads to unrealistic results if a logarithmic Γ grid is used to analyze autocorrelation functions originating from relaxation processes covering a wide range of Γ values. This problem is overcome by setting the parameter IQUAD = 1.¹⁹ In this case the distribution of relaxation rates is expressed as $[\Gamma A(\Gamma)]$ as function of $\log(\Gamma)$.²⁰

From plots of $[\Gamma A(\Gamma)]$ versus Γ the maximum values of Γ (i.e., $\Gamma_{\text{max},i}$, $i = 1, 2$, or 3) are obtained. If no angular dependence is observed, the apparent diffusion coefficient D is identified with the mean value of $(\Gamma_{\text{max}}/q^2)$. In the case of a nonzero slope of the $(\Gamma_{\text{max}}/q^2)$ versus q^2 curves, the value D is calculated from the intercept of a linear extrapolation [$D = \lim_{q^2 \rightarrow 0} (\Gamma_{\text{max}}/q^2)$].

The dynamic light scattering experiments are carried out using aqueous solutions of polyelectrolytes with $0.09 \leq \alpha_e \leq 0.46$ at concentrations \bar{c}_p in the range $0.1 \bar{c}^+ < \bar{c}_p < 27\bar{c}^+$ ($\bar{c}^+ = 1 \text{ g dm}^{-3}$) and $c_s = 1 \times 10^{-2} \text{ c}^+$. This corresponds to a range of the reduced variable $\Lambda (= \alpha_e c_m/c_s)$ of $0.03 \leq \Lambda \leq 8.0$. For different samples the polyelectrolyte concentrations are adjusted to give the same values of the dimensionless variable Λ .

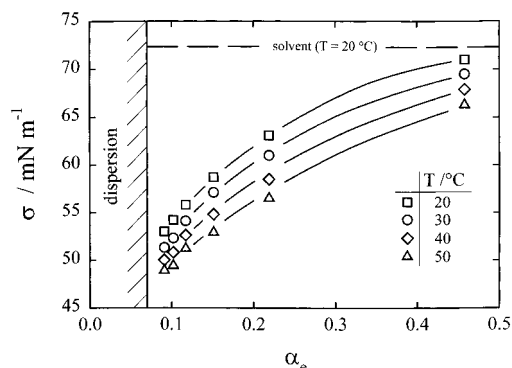


Figure 1. Surface tension σ of aqueous solutions of P2VP quaternized with ethyl bromide to different extents as a function of the degree of quaternization α_e (α_e : 0.09, 0.10, 0.12, 0.15, 0.22, 0.46; $\bar{c}_p = 1\bar{c}^+$; c_s (KBr) = $1 \times 10^{-2}\bar{c}^+$; $\bar{c}^+ = 1 \text{ g dm}^{-3}$; $\bar{c}^+ = 1 \text{ mol dm}^{-3}$). Parameter: T , temperature. Solvent: aqueous solution of KBr.

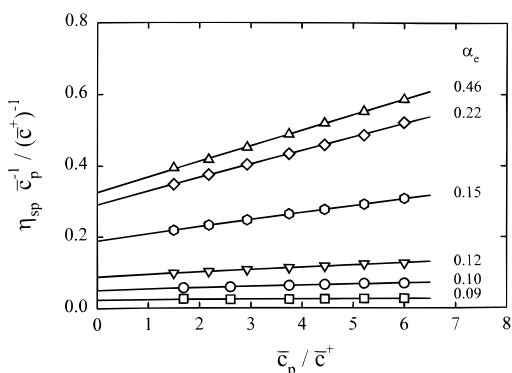


Figure 2. Reduced viscosity η_{red} ($=\eta_{sp}/\bar{c}_p$) of aqueous solutions of P2VP quaternized with ethyl bromide to different extents as a function of the polyelectrolyte concentration \bar{c}_p (η_{sp} , specific viscosity, $\eta_{sp} = (\eta - \eta_0)/\eta_0$; η and η_0 , viscosities of the solution and the solvent, respectively; c_s (KBr) = $1 \times 10^{-2}\bar{c}^+$; T , temperature, $T = 25.00 \pm 0.05$ °C; parameter, degree of quaternization α_e).

3. Results and Discussion

3.1. Surface Tension. Values of the surface tension σ of aqueous polyelectrolyte solutions with a concentration $\bar{c}_p = 1\bar{c}^+$ are shown in Figure 1 as a function of the degree of quaternization α_e . Parameter is the temperature (20 °C $\leq T \leq 50$ °C). The results reflect an increase of the hydrophilic properties of the polyelectrolytes with increasing values of α_e .

P2VP is not soluble in water. P2VP with a degree of quaternization of $\alpha_e = 0.09$ can be dissolved in an aqueous KBr solution of $c_s = 1 \times 10^{-2}\bar{c}^+$. At this value of α_e the mean distance between charged pyridinium groups is $\langle L \rangle = 2.8$ nm (see Table 1) corresponding to a length of a hydrocarbon chain of about $n = 19$ carbon atoms. It is found that this polyelectrolyte has surface-active properties in aqueous solutions (see Figure 1). For $\alpha_e = 0.46$ the mean distance between pyridinium groups along a P2VP chain has a value $\langle L \rangle = 0.5$ nm (see Table 1) corresponding to a hydrocarbon chain of $n = 3$ carbon atoms. This polyelectrolyte is only slightly surface active (see Figure 1).

3.2. Viscosity. Results of the viscosity measurements are shown in Figure 2. It is assumed that for the salt concentration used the shear viscosity is independent of the shear rate in the range of S_{eff} values used in this study ($250 \text{ s}^{-1} \leq S_{eff} \leq 1150 \text{ s}^{-1}$).²¹ The slope and the intercept of the straight lines increase with increasing charge density of the polyelectrolytes. From the observed linearity of the η_{red} versus \bar{c}_p curves,

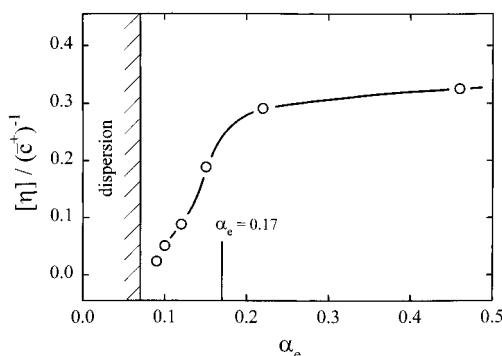


Figure 3. Intrinsic viscosity $[\eta]$ ($=\lim \bar{c}_p \rightarrow 0 (\eta_{red})$) of aqueous solutions of P2VP quaternized with ethyl bromide to different extents as a function of the degree of quaternization α_e ($1.5\bar{c}^+ \leq \bar{c}_p \leq 6.0\bar{c}^+$; $\bar{c}^+ = 1 \text{ g dm}^{-3}$; $c_s = 1 \times 10^{-2}\bar{c}^+$; $\bar{c}^+ = 1 \text{ mol dm}^{-3}$).

it is concluded that possible contributions of conformational changes of the macroion within the range of concentration studied on η_{red} can be neglected.²² In Figure 3 the values of the intrinsic viscosity $[\eta]$ ($=\lim \bar{c}_p \rightarrow 0 (\eta_{red})$) are plotted as a function of the degree of quaternization α_e . For values $\alpha_e \leq 0.15$ the intrinsic viscosity decreases with decreasing α_e , whereas the change of $[\eta]$ is comparatively small for $\alpha_e > 0.15$.

The characteristic features of the surface tension and the viscosity measurements can be interpreted on a similar basis. It is assumed that the observed change of $[\eta]$ is caused by a transition from a more extended conformation of the polyelectrolyte chains existing at $\alpha_e > 0.15$ to a more coiled up conformation at lower values of α_e ($\alpha_e \leq 0.15$). This transition could be caused by intramolecular hydrophobic interactions between hydrophobic sections of the hydrocarbon backbone which exist at low values of α_e . The influence of intermolecular electrostatic effects on the viscosity can be neglected at a salt concentration of $c_s = 1 \times 10^{-2}\bar{c}^+$.²³ Monte Carlo simulations of hydrophobic polyelectrolytes show that a transition from a collapsed chain at low charge densities to an expanded chain at high charge densities can be explained purely on the basis of an intramolecular competition between Coulombic and hydrophobic interactions.²⁴

3.3. Dynamic Light Scattering. Analysis of the Autocorrelation Function. Autocorrelation functions typical for the systems studied are shown in a previous report.¹⁰ The analysis of the $g^{(1)}(\tau)$ data using Provencher's program CONTIN gives the following results (see Figure 4):

(a) For $\Lambda \leq 0.2$ the distribution $A(\Gamma)$ is monomodal independently of the value α_e . The width of the distribution does not change measurably with α_e .

(b) For $0.2 \leq \Lambda < 1$ ($0.09 \leq \alpha_e \leq 0.46$) and for $\alpha_e \geq 0.16$ and $\Lambda \geq 1$, the distribution $A(\Gamma)$ is bimodal. Two well-separated peaks are observed, reflecting two dynamic processes ("fast mode", relaxation time τ_f ; "slow mode", relaxation time τ_s). This behavior is typical for aqueous solutions of highly charged polyelectrolytes in the presence of salt.^{1,4,6} It has also been found in P2VP solutions with a broad molar mass distribution quaternized with ethyl bromide to small extents ($0.11 \leq \alpha_e \leq 0.46$).¹⁰ There are reports in the literature that the same is true for solutions of weakly charged polyelectrolytes with no added salt (poly(methylacrylic acid) partially neutralized with NaOH and P2VP partially protonated with HCl).^{8,9}

(c) For $\Lambda \geq 1$ and $0.09 \leq \alpha_e \leq 0.15$ the distribution is trimodal (fast mode, τ_f ; "intermediate mode", τ_{int} ; slow mode, τ_s ; $\tau_f < \tau_{int} < \tau_s$). The amplitude of the "interme-

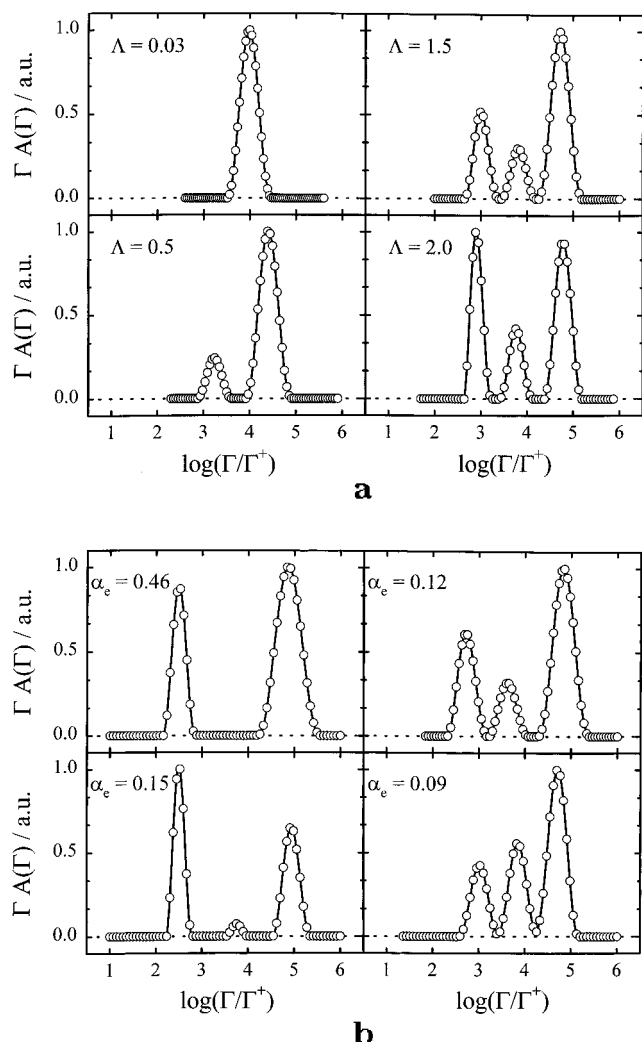


Figure 4. Results of the analysis of $g^{(1)}(\tau)$ data using the program CONTIN: Plot of the distribution function $[\Gamma A(\Gamma)]$ of the relaxation rate Γ (scattering angle θ , $\theta = 90^\circ$; $\Gamma^+ = 1 \text{ s}^{-1}$). The data refer to aqueous solutions of quaternized P2VP in the presence of salt ($c_s = 1 \times 10^{-2} \text{ c}^+$). The polyelectrolyte solutions are characterized by (a) $\alpha_e = 0.10$; parameter, Λ ; (b) $\Lambda = 2.0$; parameter, α_e .

diated" mode increases with decreasing values of α_e . The diffusive modes of the polyelectrolyte solutions observed in this study are summarized in Figure 5 using the variables α_e and Λ .

(d) The diffusive modes differ in their q^2 -dependence. The fast and intermediate modes show no dependence on q^2 in the entire range of the Λ values studied using samples with different values of α_e . For the slow mode, plots of $\Gamma_{\text{max},s}/q^2$ versus q^2 have positive slopes.^{4,8}

Apparent Diffusion Coefficient. Figure 6 shows a double-logarithmic plot of D as a function of the reduced variable Λ . The fast mode (D_f) increases with increasing values of Λ starting around $\Lambda \approx 0.3$. The intermediate diffusive mode (D_{int}) is observed for α_e values in the range $0.09 \leq \alpha_e \leq 0.15$ for $\Lambda \geq 1$. D_{int} is constant within the uncertainty of the experiments. The slow mode (D_s) appears at the value $\Lambda \approx 0.3$ for all polyelectrolytes studied ($0.09 \leq \alpha_e \leq 0.46$). The value D_s decreases with increasing polyelectrolyte concentration.

"Slow Mode". The physical origin of the slow diffusive process is not understood yet.²⁵⁻³⁰ There are reports in the literature that the presence of the slow mode as well as the distribution of relaxation rates $A(\Gamma)$ depends on the treatment of the solutions.²⁵ In this

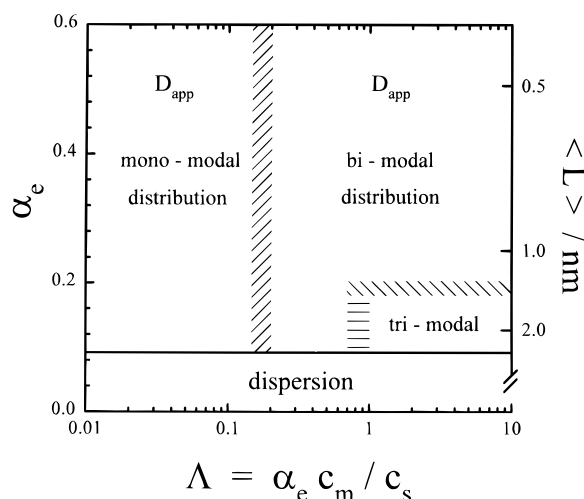


Figure 5. "Phase diagram" of the diffusive modes observed by dynamic light scattering experiments with aqueous solutions of P2VP quaternized with ethyl bromide to different degrees of quaternization α_e ($0.09 \leq \alpha_e \leq 0.46$; $T = 25.000 \pm 0.001^\circ \text{C}$). The results are plotted as a function of Λ ($=\alpha_e c_m / c_s$; c_m , molar volume concentration of the repeat unit of the polymer; c_s , electrolyte concentration; $c_s = 1 \times 10^{-2} \text{ c}^+$). On the axis of the right-hand side, the values of the mean distance $\langle L \rangle$ between the quaternized monomers along the polymer chain are indicated.

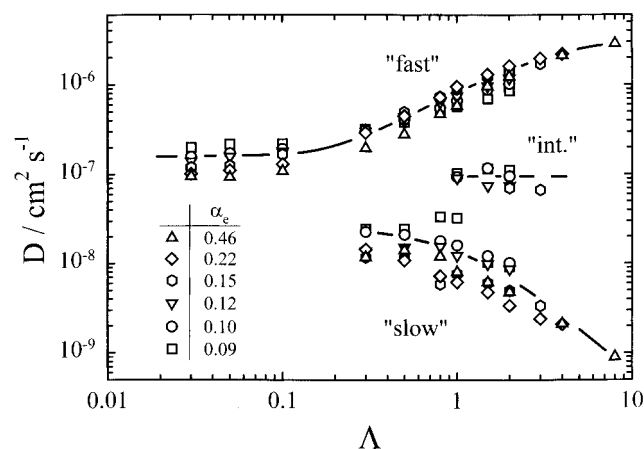


Figure 6. Double-logarithmic plot of the fast (index f), intermediate (index int), and slow (index s) apparent diffusion coefficients (D_f , D_{int} , and D_s) as function of the reduced composition variable Λ ($=\alpha_e c_m / c_s$; $c_s = 1 \times 10^{-2} \text{ c}^+$).

study the influence of filtration on the slow mode in polyelectrolyte solutions with $\alpha_e = 0.09$ and $\alpha_e = 0.46$ is checked for Λ values of $\Lambda = 0.03$ and 2.0 . The solutions were filtered through pore-controlled polycarbonate filters with pore sizes 0.1 and $0.2 \mu\text{m}$. The presence of the slow mode and its distribution of relaxation rates $A(\Gamma)$ is not influenced by this treatment. After filtration no change of $A(\Gamma)$ with time is found (time period, up to 7 weeks).

According to Sedlak the slow mode is not caused by intermolecular hydrophobic interactions.³¹ This observation is confirmed by the results of this study: The amplitude $A(\Gamma)$ of the slow mode does not increase with increasing hydrophobicity of the polyelectrolytes (decreasing values of α_e in the range $0.09 \leq \alpha_e \leq 0.46$).

"Intermediate Mode". The intermediate mode is observed when the number of carbon atoms between two charged groups exceeds a value $n \geq 12$ (i.e., $\alpha_e \leq 0.15$; $\langle L \rangle \geq 1.7 \text{ nm}$). This corresponds to the range of α_e in which characteristic changes of the surface tension and the intrinsic viscosity are observed ($\alpha_e \leq 0.15$). On the

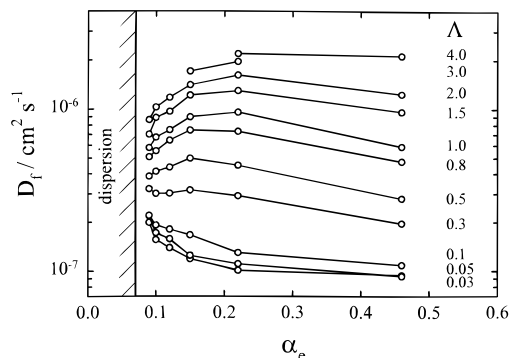


Figure 7. Dependence of the fast apparent diffusion coefficient D_f on the degree of quaternization α_e at constant values of the reduced variable Λ ($=\alpha_e c_m / c_s$).

basis of these findings, it is assumed that the intermediate mode is caused by the dynamics of intramolecular hydrophobic regions.

The existence of a third intermediate mode also shows up in dynamic light scattering data obtained with aqueous solutions of P4VP completely quaternized with dodecyl bromide and ethyl bromide in varying ratios ($0.01 \leq \alpha_d \leq 0.19$, $\alpha_e = 1 - \alpha_d$) in the presence of salt.¹³

“Fast Mode”. It is generally accepted that the fast mode reflects the diffusive properties of single macroions or at least large segments of single macroions. The dependence of D_f on Λ with $0.09 \leq \alpha_e \leq 0.46$ is similar to that reported by Förster et al. with high-charge-density P2VP–benzyl bromide polyelectrolytes ($0.40 \leq \alpha_b \leq 1.00$) in KBr solution.⁴ This behavior is also found with P2VP–ethyl bromide polyelectrolytes with a broad molar mass distribution ($M_w = 3.74 \times 10^5$; $M_w/M_n = 2.24$; $0.08 \leq \alpha_e \leq 0.46$).¹⁰

A plot of D_f as a function of α_e with Λ as a parameter (see Figure 7) reveals that the characteristics of the dependence of D_f on α_e changes with Λ . This could be the cause of conflicting results reported in the literature about the dependence of D_f on the charge density of the polyelectrolytes.^{8,9}

An extension of the scaling theory originally developed to explain the properties of neutral polymers to polyelectrolyte solutions predicts a power law behavior of the concentration dependence of the diffusion coefficient D ($=D_f$) at polyelectrolyte concentrations above an overlap concentration (i.e., $c_m > c_m^*$, $D \sim (c_m)^\nu$ with $\nu = 3/4$).^{32–34} Experimental data obtained with aqueous sodium poly(styrenesulfonate) in the presence of salt are consistent with the theoretical prediction.³⁵ Recently, values of $\nu > 3/4$ have been reported with aqueous solutions of protonated poly(ethylene imine).³⁶

We have analyzed our data in terms of this concept by plotting the ratio (D_f/D_f^0) as a function of c_m in a double-logarithmic plot (see Figure 8). α_e is a parameter. For a better presentation of the data the values of D_f are divided by D_f^0 which is the value of D_f in the plateau region of the double-logarithmic $D(\Lambda)$ diagram (low values of Λ , e.g., $\Lambda = 0.03$). It is found that the range of concentrations c_m ($0.01c^+ < c_m < 0.3c^+$) in which D_f follows a power law ($D_f \sim (c_m)^\nu$) decreases with increasing values of α_e . The exponent ν is a function of α_e ($\alpha_e = 0.09$, $\nu \approx 0.52$; $\alpha_e = 0.46$, $\nu \approx 1.1$). This is not predicted by the theory. The theoretically predicted value $\nu = 3/4$ lies in the range of the experimentally found values ($0.52 < \nu < 1.1$).

According to the scaling concept, the value of c_m above which D_f can be represented by a power law ($D_f \sim (c_m)^\nu$) is given by the overlap concentration c_m^* . It can be calculated from an expression given by Dobrynin et al.

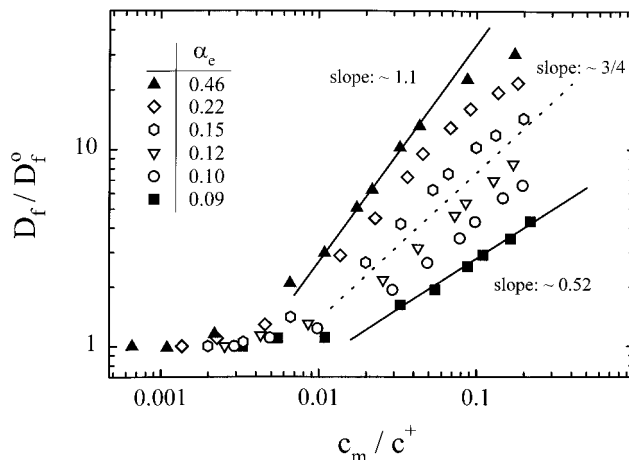


Figure 8. Double-logarithmic plot of the ratio D_f/D_f^0 as a function of the molar volume concentration of the repeat unit of the polymer c_m ($D_f^0 = D_f$ ($\Lambda = 0.03$); see Figure 6).

(see eq 2). A is the number of monomers between two

$$c_m^*(1 + 2Ac_s/c_m^*)^{-3/2} \approx N_L^{-1}N^{-2}(B/l_0)^3 \quad (2)$$

charged monomers, $A = 1/\alpha_e$, and N_L is Avogadro's number, N is the degree of polymerization, and B the ratio of the contour length and the actual length of the chain.³⁴

The parameter B is calculated for the Θ -temperature of the uncharged chain ($B = [A^2/(l_B l_0)]^{1/3}$; l_B , Bjerrum length, $l_B = 0.71$ nm; l_0 , length of a repeat unit, $l_0 = 0.25$ nm). For values of α_e in the range $0.09 \leq \alpha_e \leq 0.46$ the calculated values for c_m^* are in the range $2 \times 10^{-2}c^+ \geq c_m^* \geq 2.5 \times 10^{-3}c^+$. This is the range of c_m in which D_f increases in a double-logarithmic D_f/D_f^0 versus c_m plot (see Figure 8).

The dependence of the apparent diffusion coefficient D_f on the polyion concentration and the salt concentration can be described by a model worked out by Lee and Schurr.^{5,6} It is based on the assumption that the thermal motion of the polyions is coupled with that of the counterions and the co-ions present in the solution. The model gives a relation between the apparent diffusion coefficient D_{app} ($=D_f$) and the diffusion coefficients of the polyion D_p and of the salt D_{salt} ($=D_+ = D_-$; (+) K^+ ; (–) Br^- ; see eqs 3 and 4). D_{app} refers to the apparent diffusion coefficient from dynamic light scattering data extrapolated to $q^2 \rightarrow 0$.

$$D_{app} = 1/2\{D_p(1 - \Omega) + D_{salt}(1 + \Omega)\} \quad (3)$$

with

$$\Omega = \frac{Z_{eff}D_p - D_{salt}\{1 + 2c_s/(c_p Z_{eff})\}}{Z_{eff}D_p + D_{salt}\{1 + 2c_s/(c_p Z_{eff})\}} \quad (4)$$

c_p is the molar volume concentration of the polyions and c_s that of the electrolyte. Z_{eff} is the effective number of charges of a polyion.

Equations 3 and 4 are used to describe the experimentally observed dependence of D_f obtained with P2VP–ethyl bromide polyelectrolytes of low charge density in the presence of salt. Equation 4 suggests to introduce a dimensionless variable $\Lambda_{eff} = Z_{eff}c_p/c_s$ defined similar to Λ ($=\alpha_e c_m / c_s$). The analysis of experimental data is divided into two parts: experimental data obtained with samples of small degrees of quaternization (α_e : 0.09, 0.10, 0.12) and with higher values of α_e (α_e : 0.15, 0.22, 0.46). Equation 3 is fitted to the first

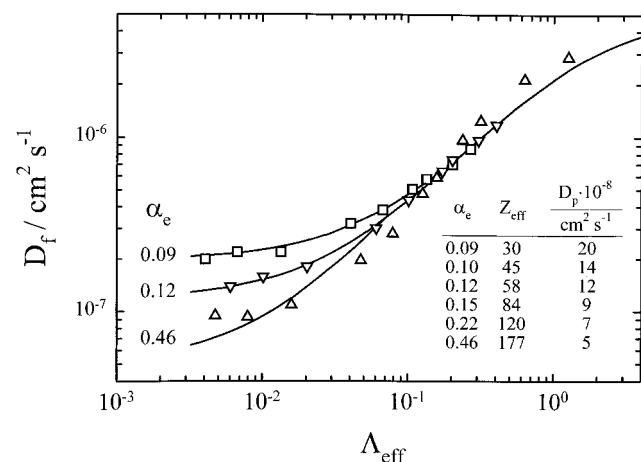


Figure 9. Comparison of $D_f(\Lambda_{\text{eff}})$ curves calculated from the Lee-Schurr model (see eqs 3 and 4) with the experimental values. Drawn out line: calculated curves. The data points refer to experimental results obtained for three samples with different degrees of quaternization α_e (α_e : 0.09, 0.12, 0.46; fixed parameter values, $D_{\text{salt}} = 2.0 \times 10^{-5} \text{ cm}^2 \text{ s}^{-1}$, $c_s = 1 \times 10^{-2} \text{ c}^+$). The values for Z_{eff} and D_p obtained from the fits to the $D_f(c_p)$ data of each sample studied are shown in the figure (free parameters of the fit: Z_{eff} and D_p for α_e : 0.09, 0.10, 0.12; Z_{eff} for α_e : 0.15, 0.22, 0.46).

group of $D_f(c_p)$ data with two free parameters (Z_{eff} , D_p) and two fixed parameters (c_s , D_{salt}). The value of c_s is given by the experimental conditions ($c_s = 1 \times 10^{-2} \text{ c}^+$). A typical value of D_{salt} for KBr is taken from the literature ($D_{\text{salt}} = 2.0 \times 10^{-5} \text{ cm}^2 \text{ s}^{-1}$).³⁷ For the second group of $D_f(c_p)$ data the free parameters are reduced to Z_{eff} . D_p is fixed. This is necessary to obtain stable values of the fitting parameters. Figure 9 shows the results of such fits for three samples (α_e : 0.09, 0.12, 0.46). The experimental $D_f(\alpha_e, c_p, c_s)$ data are satisfactorily described by eq 3. The values of Z_{eff} obtained from the fits are ≈ 5 –7 times smaller than those calculated from the degree of quaternization (see Table 1). This has been found also by others in the analysis of experimental data obtained with highly charged polyelectrolytes.^{38,39}

The section of the D_f versus Λ_{eff} curves in which D_f increases with increasing values of Λ_{eff} (i.e., $\Lambda_{\text{eff}} > 0.1$) collapses for the entire range of α_e studied. This indicates that the increase of D_f with the polyelectrolyte concentration can be described by taking into account only the electrostatic coupling between small ions and polyions and neglecting the polymer properties. A change of the hydrophobic/hydrophilic balance associated with a variation of α_e apparently has no influence on the concentration dependence of D_f .

4. Conclusions

The dynamic properties of P2VP quaternized with ethyl bromide to different small extents ($0.09 \leq \alpha_e \leq 0.46$; α_e , degree of quaternization with ethyl bromide) and dissolved in an aqueous solution of KBr ($c_s = 10^{-2} \text{ c}^+$) show the typical behavior of aqueous solutions of polyelectrolytes of high charge density (i.e., the existence of fast and slow diffusive modes). The $D(\alpha_e, c_p)$ data scale when they are plotted as a function of the reduced variable Λ ($=\alpha_e c_p / c_s$). Polyelectrolytes containing long hydrophobic segments ($\alpha_e \leq 0.15$) show a third diffusive mode for $\Lambda \geq 1$ besides the fast and slow diffusive modes. This process is assumed to reflect the dynamic properties of hydrophobic domains.

The coupled mode theory of the dynamics of polyelectrolytes in solution describes the concentration depend-

ence of the fast diffusion coefficient for the charge densities studied ($0.09 \leq \alpha_e \leq 0.46$). The variable Λ_{eff} ($=Z_{\text{eff}} c_p / c_s$) is suited to scale the influence of electrostatic coupling between the polyions and the counterions (c_p , molar polyelectrolyte concentration). Λ_{eff} can be replaced by Λ ($=\alpha_e c_m / c_s$) when the mean distance between the charges along the polymer chain exceeds the Bjerrum length (c_m , molar concentration of the repeat unit).

Acknowledgment. We thank H. Ruf (Max-Planck-Institut of Biophysics, Frankfurt/Main, Germany) for his help with particular features of the program CONTIN. The financial support of the Deutsche Forschungsgemeinschaft (DFG) is gratefully acknowledged.

References and Notes

- (1) Schmitz, K. S. *Macroions in Solution and Colloidal Suspension*; VCH: New York, 1993.
- (2) Mandel, M. In *Dynamic Light Scattering, The Method and Some Applications*; Brown, W., Ed.; Clarendon Press: Oxford, U.K., 1993; pp 319–371.
- (3) Förster, S.; Schmidt, M. *Adv. Polym. Sci.* **1995**, *120*, 51.
- (4) Förster, S.; Schmidt, M.; Antonietti, M. *Polymer* **1990**, *31*, 781.
- (5) Lee, W.; Schurr, J. M. *J. Polym. Sci.* **1975**, *13*, 873.
- (6) Lin, S.-C.; Lee, W.; Schurr, J. M. *Biopolym.* **1978**, *17*, 1041.
- (7) Manning, G. S. *J. Chem. Phys.* **1969**, *51*, 924.
- (8) Walkenhorst, R.; Dorfmueller, Th.; Eimer, W. *Ber. Bunsen-Ges. Phys. Chem.* **1995**, *99*, 1137.
- (9) Sedlak, M.; Konak, C.; Stepanek, P.; Jakes, J. *Polymer* **1987**, *28*, 873.
- (10) Topp, A.; Belkoura, L.; Woermann, D. *Ber. Bunsen-Ges. Phys. Chem.* **1995**, *99*, 730.
- (11) Strauss, U. P.; Williams, B. L. *J. Phys. Chem.* **1961**, *65*, 1390.
- (12) Laschewsky, A. *Adv. Polym. Sci.* **1995**, *124*, 1.
- (13) Gröhn, F.; Topp, A.; Belkoura, L.; Woermann, D. *Ber. Bunsen-Ges. Phys. Chem.* **1995**, *99*, 736.
- (14) (a) Kroeplin, W. *Kolloid. Z.* **1929**, *47*, 294. (b) Dinsdale, A.; Moore, F. *Viscosity and its Measurement*; Chapman and Hall Ltd.: London, 1962. (c) Oxtoby, D. W. *J. Chem. Phys.* **1975**, *62*, 1463.
- (15) Oswald, U.; Belkoura, L.; Jungk, M.; Woermann, D. *Ber. Bunsen-Ges. Phys. Chem.* **1984**, *88*, 635.
- (16) Provencher, S. W. *Comput. Phys. Commun.* **1982**, *27*, 213.
- (17) Provencher, S. W. *Comput. Phys. Commun.* **1982**, *27*, 229.
- (18) Provencher, S. W. CONTIN Users Manual. EMBL Technical Report DA05; European Molecular Biology Laboratory, 1982.
- (19) Ruf, H., private communication.
- (20) Stepanek, P. In *Dynamic Light Scattering, The Method and Some Applications*; Brown, W., Ed.; Clarendon Press: Oxford, U.K., 1993; pp 177–241.
- (21) Yamanaka, J.; Araie, H.; Matsuoka, H.; Kitano, H.; Ise, N.; Yamaguchi, T.; Saeki, S.; Tsubokawa, M. *Macromolecules* **1991**, *24*, 3206.
- (22) Eisenberg, H.; Pouyet, J. *J. Polym. Sci.* **1954**, *13*, 85.
- (23) Yamanaka, J.; Yamada, S.; Ise, N.; Yamaguchi, T. *J. Polym. Sci.* **1995**, *33*, 1523.
- (24) Hooper, H. H.; Beltram, S.; Sassi, A. P.; Blaras, H.; Prausnitz, J. M. *J. Chem. Phys.* **1990**, *93*, 2715.
- (25) Ghosh, S.; Peitzsch, R.; Reed, W. F. *Biopolymers* **1992**, *32*, 1105.
- (26) Reed, W. F. *Macromolecules* **1994**, *27*, 873.
- (27) Sedlak, M. *Macromolecules* **1993**, *26*, 1158.
- (28) Sedlak, M. *ACS Symp. Ser.* **1994**, *548*, 337.
- (29) Sedlak, M. *Macromolecules* **1995**, *28*, 793.
- (30) Schmitz, K. S. *Macromol. Symp.* **1994**, *79*, 57.
- (31) Sedlak, M. *J. Chem. Phys.* **1994**, *101*, 10140.
- (32) de Gennes, P.-G.; Pincus, P.; Velasco, R. M.; Brochard, F. *J. Phys. Fr.* **1976**, *37*, 1461.
- (33) Odijk, T. *Macromolecules* **1979**, *12*, 688.
- (34) Dobrynin, A. V.; Colby, R. H.; Rubinstein, M. *Macromolecules* **1995**, *28*, 1859.
- (35) Koene, R. S.; Mandel, M. *Macromolecules* **1983**, *16*, 227.
- (36) Smits, R. G.; Kuil, M. E.; Mandel, M. *Macromolecules* **1993**, *26*, 6808.
- (37) Schäfer, K. *Landolt-Börnstein, Zahlenwerte und Funktionen*; Springer-Verlag: Berlin, 1969.
- (38) Ramsay, D. J.; Schmitz, K. S. *Macromolecules* **1985**, *18*, 2422.
- (39) Wang, L.; Garner, M. M.; Yu, H. *Macromolecules* **1991**, *24*, 2368.